Published in final edited form as:
Environ Sci Technol. 2019 September 03; 53(17): 10329–10341. doi:10.1021/acs.est.9b02448.

In Vitro, *in Vivo,* and Spectroscopic Assessment of Lead Exposure Reduction via Ingestion and Inhalation Pathways Using Phosphate and Iron Amendments

Farzana Kastury[a,*], **Euan Smith**[a], **Emmanuel Doelsch**[a,b,h], **Enzo Lombi**[a], **Martin Donnelley**[c,d], **Patricia L. Cmielewski**[c,d], **David W. Parsons**[c,d], **Kirk G. Scheckel**[e], **David Paterson**[f], **Martin D. de Jonge**[f], **Carina Herde**[g], **Albert L. Juhasz**[a]

[a]Future Industries Institute, University of South Australia, Adelaide 5095, Australia

[b]CIRAD, UPR Recyclage et risque, F-34398 Montpellier, France

[c]Women's and Children's Hospital, Adelaide 5006, Australia

[d]Adelaide Medical School and Robinson Research Institute, University of Adelaide, Adelaide 5000, Australia

[e]United States Environmental Protection Agency, Cincinnati 45224, United States

[f]Australian Synchrotron, ANSTO, Clayton 3168, Australia

[g]South Australian Health and Medical Research Institute, Adelaide 5086, Australia

[h]Recyclage et Risque, Univ Montpellier, CIRAD, Montpellier, France

Abstract

This study compared lead (Pb) immobilization efficacies in mining/smelting impacted soil using phosphate and iron amendments via ingestion and inhalation pathways using *in vitro* and *in vivo* assays, in conjunction with investigating the dynamics of dust particles in the lungs and gastro-intestinal tract via X-ray fluorescence (XRF) microscopy. Phosphate amendments [phosphoric acid (PA), hydroxyapatite, monoammonium phosphate (MAP), triple super phosphate (TSP), and bone meal biochar] and hematite were applied at a molar ratio of Pb:Fe/P = 1:5. Pb phosphate formation was investigated in the soil/post-*in vitro* bioaccessibility (IVBA) residuals and in mouse lung via extended X-ray absorption fine structure (EXAFS) and X-ray absorption near edge structures (XANES) spectroscopy, respectively. EXAFS analysis revealed that anglesite was the dominant phase in the ingestible (<250 μm) and inhalable (<10 μm) particle fractions. Pb IVBA was significantly reduced ($p < 0.05$) by phosphate amendments in the <250 μm fraction (solubility bioaccessibility research consortium assay) and by PA, MAP, and TSP in the <10 μm fraction (inhalation–ingestion bioaccessibility assay). A 21.1% reduction in Pb RBA (<250 μm fraction) and 56.4% reduction in blood Pb concentration (<10 μm fraction) were observed via the ingestion and inhalation pathways, respectively. XRF microscopy detected Pb in the stomach within 4 h, presumably via mucociliary clearance.

* farzana.kastury@mymail.unisa.edu.au.

Graphical Abstract

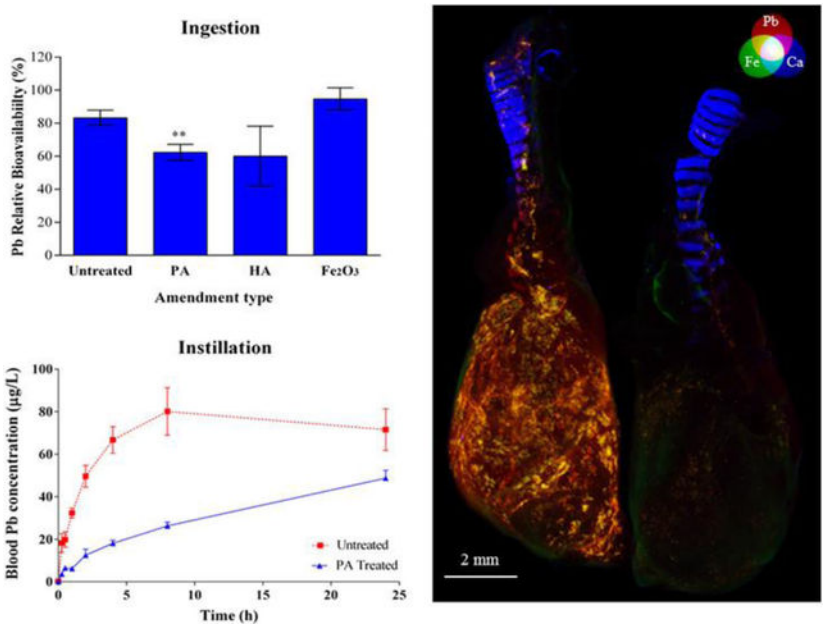

1. Introduction

Lead (Pb) exposure has been linked with approximately half a million deaths and nine million disability-adjusted life years worldwide by the Institute for Health Metrics and Evaluation.(1) Cognitive and neurological impairment due to childhood Pb exposure is well documented(2–4) and can occur at blood Pb concentrations (PbB) as low as 3 μg/dL.(5) The two significant pathways for Pb exposure in humans are incidental ingestion of soil/soil borne dust and inhalation of resuspended indoor surface/house dust.(6) Solubilization of Pb occurs in the stomach acid (pH 1.5–2.5)(7,8) following soil ingestion or in lung surfactants and epithelial fluid (pH 7.0)(9) following dust inhalation. The proposed mechanisms for Pb absorption include passive and facilitated diffusion via the divalent metal transporter in the lungs, duodenum, and ileum of the small intestine (pH 7.0).(10–12) Children are the most at risk of Pb exposure from soil ingestion or dust inhalation because of their higher occurrence of hand-to-mouth activities(7), as well as due to their increased respiratory frequency, leading to a higher deposition fraction of fine particulate matter (<4 μm) in the respiratory tract.(13,14)

Reduction in Pb absorption into the systemic circulation using soil amendments (e.g., phosphates, metal oxides, clay minerals) may be a cost-effective risk mitigation strategy compared to soil removal, replacement, washing, and capping.(7,15) In particular, phosphate amendments may reduce Pb bioavailability by promoting the formation of poorly soluble Pb phosphate species [e.g., pyromorphites ($Pb_5(PO_4)_3X$, where X = OH/Cl/F) and $Pb_3(PO_4)_2$]. (7,15,16) Although Pb immobilization has been demonstrated in humans(17) and animal-feeding studies,(15,17,18) its efficacy is governed by site-specific soil chemistry, Pb speciation, and choice of amendment.(7)

The predominant focus for Pb immobilization studies thus far has been demonstrating reduction of Pb bioavailability (absorption of Pb into systemic circulation) or bioaccessibility (dissolution of Pb in simulated biological solutions) via the ingestion pathway. During the analysis of oral bioavailability/bioaccessibility, the <250 μm soil particle fraction is generally used. However, Pb-contaminated particulate matter with <10 μm in aerodynamic diameter (PM_{10}) may be inhaled in arid mining/smelting impacted regions due to resuspension of dust inside or near households in the vicinity of the mining region.(19–21) The concentration of Pb (as well as other toxic elements present) may be several orders of magnitude higher in the <10 μm particle fraction compared to the <250 μm counterpart.(22) Although the mass of inhaled dust may be less than the mass that is incidentally ingested (depending on the local concentration of particulate matter), Fent et al. (19) reported that Pb bioavailability from contaminated soil via instillation in rodent lung was significantly higher than ingestion when identical doses for both pathways were used. When deposited in the respiratory system, rapid Pb absorption from the lungs instilled with Pb-acetate or Pb contaminated soil may occur,(19) presumably due to the high gas exchange surface area (70 m^2), short distance between the air–blood barrier (0.5 μm), and high vascularization of the respiratory system.(23) Additionally, particles may reach the gastro-intestinal (GI) tract via the mucociliary escalator and further dissolve in the stomach, be absorbed in the intestine,(24) translocate to extra-pulmonary organs (e.g., liver, heart, bone), be retained in the lung for weeks to years,(25) and exert additional acute or systemic toxicity.(12,26) Therefore, incorporating Pb immobilization information for both ingestion and inhalation pathways may be considered a holistic approach when recommending an amendment strategy for risk minimization in arid regions.

Discovered in 1883, Broken Hill, Australia contains the world's largest Pb, zinc (Zn), and silver (Ag) ore deposit known as the Line of Lode.(27) In addition to the continuous mining since discovery, a brief period of Pb and Zn smelting (1883–1898)(27) resulted in widespread Pb contamination in urban residential areas of the Broken Hill.(28) Dust suppression and Pb exposure mitigation strategies in Broken Hill residential regions to date include the application of cracker dust in parts of the central southern urban area(29) and home remediation trials (encapsulation/removal of dust, sealing of cracks in the windows/walls).(20) However, a high risk of chronic childhood Pb exposure was predicted in a recent study by Yang and Cattle.(28)

This study determined the efficacy of Pb immobilization via ingestion and inhalation pathways in Pb contaminated soil from Broken Hill using P and Fe amendments. In addition to assessing Pb exposure reduction using bioaccessibility and bioavailability, changes in Pb speciation in the pre- and postbioaccessibility residuals and in the lungs were determined using extended X-ray absorption fine structure (EXAFS) and X-ray absorption near edge structures (XANES) spectroscopy, while Pb dynamics following *in vivo* inhalation exposure was assessed via X-ray Fluorescence (XRF) microscopy.

2. Materials and Methods

2.1. Soil Collection and Physicochemical Characterization

Mining/smelting impacted topsoil (0–20 cm) was collected from Broken Hill, Australia. After drying at 40°C, the soil was sieved to <2 mm, and its water holding capacity (WHC), pH [soil (m)/water (v) = 1:5], and total organic carbon content (LECO TrueMac CNS) were measured (n = 3). Subsamples were sieved to <250 μm (incidentally ingestible fraction) and <10 μm (inhalable or dust fraction) (Endecotts Octagon digital shaker). Each fraction (0.1 g, n = 3) and a standard reference material (SRM) from the National Institute of Standards and Technology (NIST) 2710a were predigested overnight in 5 mL aqua-regia and then digested in a MARS-6 microwave (CEM) using USEPA method 3051.(30) Digested samples were syringe filtered (0.45 μm, cellulose acetate) and diluted with Milli-Q water and the pseudototal elemental concentrations analyzed using inductively coupled plasma mass spectrometry (ICP-MS) (Agilent 8800) according to USEPA method 6020A.(31) The average recovery of Pb from SRM, check values, duplicates, and spiked samples were within the limits specified in USPEA method 6020A.(31) See the Supporting Information (SI) for further details.

2.2. Application of Amendments

Soil amendment and ageing was conducted according to Juhasz et al.(32) using phosphoric acid (PA, Fisher Scientific), hydroxyapatite (HA, Sigma-Aldrich), monoammonium phosphate (MAP, Sigma-Aldrich), triple super phosphate (TSP, Richgro), bone meal biochar (Charcoal House LLC, Crawford, NE), and synthetic hematite Fe_2O_3 (Sigma-Aldrich). See the SI for more details. After the application of amendments (Pb:P/Fe = 1:5) at 80% WHC and ageing for 2 weeks (24 ± 2°C),(32) soils were dried (40°C) and soil pH determined in a subsample. To remove excess P, soils were leached five times with natural rainwater collected from rooftop into rainwater tank (pH 5.8), followed by drying and sieving to recover the <250 μm and <10 μm particle size fractions. Pseudototal elemental concentrations from each fraction were reanalyzed as described earlier.

2.3. Assessment of InVitro Bioaccessibility (IVBA)

Oral Pb and Fe IVBA were assessed (n = 3) in the <250 μm soil particle size fraction following the Solubility Bioaccessibility Research Consortium (SBRC) assay.(33) Inhalation Pb and Fe IVBA were assessed (n = 3) in the <10 μm soil particle size fraction using the Inhalation–Ingestion Bioaccessibility Assay (IIBA)(22) using Hatch's solution.(34) Percent IVBA was calculated using eq 1 given in Kastury et al.(22) See the SI for more details.

2.4. EXAFS Assessment of Pb and Fe Speciation

Lead speciation was assessed using EXAFS in pre- and post-amendment soil as well as selected post-IVBA assay residuals (to provide speciation information on the non-bioaccessible fraction). Methodologies described in Kropf et al.(35) were used to conduct EXAFS analysis at the Materials Research Collaborative Access Team (MRCAT), Advanced Photon Source of the Argonne National Laboratory, U.S. (beamline 10-ID). See the SI for additional details.

2.5. Assessment of Oral Bioavailability via Gavage

In vivo Pb relative bioavailability (RBA) studies were conducted using female Balb/C mice (4–6 weeks old) according to the Guidelines for the Care and Use of Laboratory Animals, (36) with approval from the South Australian Health and Medical Research Institute Animal Ethics Committees (application no. SAM268). On the basis of the Pb IVBA results using SBRC assay, unamended, PA-, HA-, or Fe_2O_3-amended <250 μm soil particle fraction (20–108 μg of Pb suspended in 180 μL of Pb free water) was administered via gavage to fasted mice (20–25 g).(37) Blood (~0.5 mL) was collected via cardiac puncture 8 h post exposure, stored at 4 °C, and analyzed by ICP-MS after diluting 10-fold in blood diluent solution. (38)Equation1 according to Juhasz et al.(32) was used to calculate Pb RBA (see the SI for further details).

2.6. Assessment of Pb Bioavailability via Instillation

Based on the Pb IVBA results of IIBA, PA-amended and unamended inhalable dust (<10 μm fraction) was intratracheally instilled using female C57BL/6 mice (8–10 weeks old) with approval from the Animal Ethics Committee of the Women's and Children's Health Network, Adelaide, South Australia (WCHN AEC project No. AE1044/7/2019). Mice (n = 6) were anaesthetized and intubated,(39) and a 20 μL bolus dose (0.02 mg of dust/mL suspended in 0.9% NaCl) was administered directly into the trachea over 10 s via the endotracheal tube. Mice were exposed for 0.25, 0.5, 1, 2, 4, 8, or 24 h, after which they were humanely killed by CO_2 asphyxiation. Blood was collected via cardiac puncture, with Pb concentration analysis undertaken as described above. Lungs and the entire GI tract were removed and immediately frozen at −86 °C to prevent change in Pb speciation and stored at −80 to −20 °C until analysis.

Two sets of lungs and GI tracts for each time-point/treatment was reserved for further analysis using XRF described below, while the remaining tissues (n = 4) were used to determine Pb concentration. The GI tracts were sectioned into stomachs and intestines. Stomachs were re-frozen and freeze-dried (Modulyod Freeze-Dryer). Lungs, GI tracts, and NIST SRM 2976 were digested using nitric acid (70%) in a block digester (A.I. Scientific AIM500) ramping up to a maximum temperature of 180 °C.(40) Following digestion and evaporation of acid to ~1–2 mL, samples were diluted with Milli-Q water, syringe filtered (0.45 μm, cellulose acetate), and stored at 4°C until analyzed by ICP-MS. See the SI for more details.

2.7. XRF and XANES Analysis of Lungs and GI Tracts

In order to retain the morphology of organs during sample preparation for XRF, the mouse organs were freeze-dried (Modulyod Freeze-Dryer). The GI tracts were thawed, unraveled, and positioned onto Kapton tape, while the lungs were dissected and the left lobes were suspended on Lecter coat hangers and frozen prior to freeze-drying. The dehydrated organs were sandwiched between ultralene, and X-ray Fluorescence Microscopy (XFM) was performed (18.5 keV incident energy, velocity of 2 mm/s and a pixel size of 20 μm) at the XFM beamline at the Australian Synchrotron. Regions of interest (0.2 × 0.2 mm) from the 24 h unamended and amended lungs were selected for XANES mapping (90 energy steps,

mapped at a velocity of 0.5 mm/sec and a pixel size of 2 μm).(41) See the SI for additional details.

2.8. Statistical Analysis

To determine the efficiency of each amendment in reducing ingestion and inhalation exposure, treatment effect ratio (TER) was calculated using eq 1.

$$\mathbf{TER} = \frac{\mathbf{Pb\,IVBA}\ \text{or}\ \mathbf{RBA}\ (\%)\ \text{in amended sample}}{\mathbf{Pb\,IVBA}\ \text{or}\ \mathbf{RBA}\ (\%)\ \text{in unamended sample}} \quad (1)$$

Significant difference in Pb concentrations in soils post amendment was determined using One-Way ANOVA ($\alpha = 0.05$). Statistical significances in IVBA and RBA outcomes between unamended and amended soils were assessed using *t* test ($\alpha = 0.05$).

3. Results and Discussion

3.1. Elemental Concentration and Pb Speciation in Unamended Soil

The pH, TOC, and concentrations of elements in the bulk soil (<2 mm) and incidentally ingestible (<250 μm) and inhalable (<10 μm) soil particle fractions are listed in Table 1. The pH of the bulk soil was slightly acidic (5.2 ± 0.08) with low total organic carbon (0.5 ± 0.04%). The concentration of Pb in the <2 mm, <250 μm, and <10 μm particle size fractions were 11656 ± 754, 14874 ± 157, and 62,069 ± 739 mg/kg, exhibiting Pb enrichments of 1.3 and 5.3 fold in the <250 and <10 μm fractions, respectively. Among the other notable trace elements of interest, manganese (Mn) and zinc (Zn) were present at elevated concentrations (3334 ± 754 and 5432 ± 271 mg/kg respectively), while aluminum (Al) and iron (Fe) were the highest among the major elements (19035 ± 960 and 25746 ± 2140 mg/kg). Although metal cations, particularly Mn, Zn, and calcium (Ca), are associated with lowering PbB levels,(42,43) combined Pb and Mn exposure has been reported to exacerbate cognitive performance.(44) Similarly, when inhaled, Zn (18437 ± 174 mg/kg in the <10 μm particle fraction) may potentially cause lung inflammation and fibrosis.(45)

The predominant Pb species in the unamended <250 μm soil particle fraction was anglesite ($PbSO_4$) (66%) and organic matter bound Pb (31%), while the remainder of the Pb was mineral sorbed (e.g., adsorbed onto clays and oxides) (Table 2). Although the proportion of anglesite did not change in the <10 μm soil particle fraction (67%), the majority of the remaining Pb was distributed among clays and oxides (20%), organic matter bound Pb (8%), and plumbojarosites ($PbFe^{3+}_6(SO_4)_4(OH)_{12}$) (7%).

3.2. Effect of Soil Amendments on pH and Pb/Fe Speciation

Phosphoric acid and TSP amendments lowered soil pH from 5.2 to 3.7 and 4.8, respectively, while HA, MAP, and Fe_2O_3 amendments had a minimal effect on pH (Table S1). In contrast, biochar amendment resulted in an increase in soil pH to 6.5, presumably as a result of hydroxide ion release from biochar.(46) Speciation analysis of Pb (EXAFS) in the phosphate-amended <250 μm soil particle fractions suggested small increases in anglesites phases with corresponding decreases in organic bound Pb (Table 2). The exception was biochar, where a greater proportion of Pb was organic bound (42%), presumably due to the

interaction between Pb and organic ligands in the biochar. In the <10 μm dust fraction, minor redistribution of Pb phases between Pb adsorbed to clays and oxides and organic matter bound Pb were observed after phosphate amendment. Similar to the <250 μm soil particle fraction, biochar-amended dust was the exception, where anglesite (45%) and organic bound Pb species (42%) were the dominant Pb phases. Fe speciation in the dust fraction (Table S2) revealed that Fe was present predominantly as ferrihydrite (24–42%) and associated with clay (26–40%), with the remainder distributed as goethite (8–15%), magnetite (5–9%), hematite (5–15%), and maghemite (2–10%).

The formation of Pb phosphate species (pyromorphite and $Pb_3(PO_4)_2$) is thermodynamically favored in the presence of $H_3PO_4^0$ (at pH of <2.12) and $H_2PO_4^-$ (at pH between 2.12 to 7.21).(47) Therefore, formation of Pb phosphate species was expected following PA and TSP amendments (pH 3.7–4.8) (Table S1). However, EXAFS analysis did not detect Pb phosphates in any phosphate-amended soils for either the <250 or <10 μm soil particle size fractions, presumably because the rate of dissolution of anglesite (the dominant phase) is pH independent.(48) In the study of anglesite immobilization using $Ca(H_2PO_4)_2{\cdot}H_2O$ and HA, Cao et al.(49) and Zhang and Ryan(48) reported a rapid dissolution of anglesite in aqueous systems, with the detection of chloropyromorphite. However, more complex interactions may occur in natural soil system, limiting Pb immobilization in situ (e.g., transient increases in soluble Pb, incomplete formation, or dissolution of Pb phosphates due to inadequate Pb dissolution, and competition from high cation concentrations with phosphate for sorption sites).(50–52) Higher phosphate application rates may be necessary in future studies in Broken Hill soil to compensate for competition posed by cations (e.g., Al, Ca, Fe, Mn, and Zn).

4.0 Treatment Efficacy: Ingestion Pathway

4.1. Pb IVBA and Residual Pb Speciation Following Gastric Phase (SBRC-G) Assessment

Pb IVBA in unamended soil was 88.6 ± 0.8% when assessed in the SBRC-G phase (Figure 1A). This value was at the high end of the range (23.7–89.3%) previously reported by Yang and Cattle(28) for Broken Hill topsoil, who reported an average gastric phase Pb IVBA value of 61.2 ± 14%. The lower average value in Yang and Cattle(28) most likely reflected the assessment of soils from a large geographic area with diverse Pb speciation influencing IVBA outcomes. In contrast, soil was collected near a former Pb ore crushing area in this study and contained anglesite ($PbSO_4$) as the dominant phase, which is a common occurrence in mining impacted soils with acidic pH and results from the oxidation of galena.(7) Anglesite's solubility over a wide range of pH (2–7)(48) may have resulted in higher Pb IVBA results.

No significant reduction ($P > 0.05$; Figure 1A) in Pb IVBA was observed in P- and Fe-amended soil (TER = 1.02–1.08; Table S3) using the SBRC-G phase, which is similar to the results reported for amended mining soils when assessed at pH 1.5.(16,53,54) Pb speciation in SBRC-G residual soil identified that the majority of anglesite was solubilized (Figure 1B), which was expected due to anglesite's propensity for solubilization under low pH conditions.(48)

4.2. Pb IVBA and Residual Pb Speciation Following Intestinal Phase (SBRC-I) Assessment

When IVBA assays were modified to reflect intestinal phase conditions (i.e., addition of bile and pancreatin, pH adjustment to 7.0), Pb IVBA in the unamended soil was reduced to 16.6 ± 1.3%. The decrease in Pb IVBA corresponded to an 88% decrease in Fe IVBA (Figure S2A), resulting from the precipitation of amorphous Fe species following oversaturation of Fe during the pH change.(55) During the transition from the gastric to intestinal phases, the increase in pH may have caused Pb to precipitate and become readsorbed to the Fe oxides and/or soil matrix.(37) A corresponding increase in mineral sorbed Pb species in postextraction intestinal phase residuals (Figure 1B) supports the hypothesis that Pb co-precipitates with Fe, as suggested by Smith et al.(37) A significant reduction ($p < 0.001$) in Pb IVBA was observed for all P-amended soils (TER = 0.02–0.1). However, Pb IVBA in Fe_2O_3-amended soil was similar to the unamended soil (18.0 ± 0.7%), suggesting that Pb immobilization did not occur as a result of this amendment.

Among the phosphate-amended soils, the lowest TER following SBRC-I assessment outcome was obtained for HA- and biochar-amended soil (0.02 and 0.04, respectively), followed by PA, MAP, and TSP (TERs of 0.1). As HA and biochar exhibit low solubility in water, higher Pb/P ratios (1:5.3 and 1:4.1, respectively) were observed in the <250 μm amended soil factions following rainwater leaching used to remove the excess P after the two-week incubation period (Table S1). Consequently, due to the dissolution of P during SBRC-G assessment, higher concentrations of P were available to react with Pb in the SBRC-I phase, resulting in lower TER. This is also supported in Figure 1B, which shows a 2.2–2.3 fold increase in Pb phosphate species in the post-IVBA residuals of SBRC-I in all phosphate treated soils but not in the soil amended with Fe_2O_3. Although only PA-amended post-IVBA residual was tested to represent water-soluble amendments, presumably Pb–P would form in the MAP- and TSP-amended residuals as well.

4.3 Pb RBA

Although assessment of Pb IVBA using SBRC-I determined that all phosphate amendments were effective in reducing Pb IVBA due to the presence of Pb phosphates in the non-bioaccessible residuals, Scheckel et al.(7) cautioned the use of IVBA outcomes (extracted at pH > 1.5) in interpreting phosphate amendment efficacies due to the potential formation of pyromorphite *in vitro* as a result of the pH change. Therefore, in addition to IVBA, the efficacy of Pb immobilization was also assessed using Pb RBA in unamended and selected amended soils (PA, HA, Fe_2O_3). In the unamended soil, Pb RBA was 47.9 ± 2.6%, which was higher compared to similar studies utilizing mining/smelting impacted Australian soils.(32,37) Low Pb RBA may occur when sparingly soluble Pb species are present, such as galena or Pb phosphates.(56,57) However, the dominant Pb phase, anglesite, may have contributed to the high Pb RBA observed in this study because of its solubility in a wide pH range (2–7).(48)

When soil was amended with PA and HA, Pb RBA was reduced to 21.1 ± 6.2% (TER = 0.79) and 35.8 ± 10.7% (TER = 0.74), respectively, which supports the hypothesis of Juhasz et al.(32) that Pb immobilization may occur *in vivo*, even when *in situ* Pb phosphate

formation did not occur. Bradman et al.(18) also reported that when Pb speciation in ingested soil was compared to feces following administration in mice, Pb speciation changed during the transit through the GI tract. Despite both phosphate amendments reducing Pb RBA, a significant reduction was only observed in the PA-amended soil ($p < 0.01$). High variability in Pb RBA was observed in the HA-amended soil, which may be attributed to the slow dissolution kinetics of HA in the stomach, resulting in the formation of a layer of Pb phosphate species on the outside of the HA particles, reducing the surface area available for reactions with Pb.(48) In contrast to the P-amended sample, there was no reduction in Pb RBA in the Fe_2O_3-amended sample (TER = 1.2).

5.0 Treatment Efficacy: Inhalation Pathway

5.1. Pb IVBA and Residual Pb Speciation Following IIBA Lung Phase (IIBA-L) Assessment

In the unamended dust fraction, Pb IVBA was 61.7 ± 0.5% during the IIBA-L phase (Figure 2A). High Pb solubility in Hatch's solution was expected, given that anglesite was the dominant Pb phase with solubility in a wide pH range(48) and the high concentration of ligands and surfactants present in the extracting solution. The major speciation change in the IIBA-L phase residual was the reduction in anglesite concentration, indicating mobilization of anglesites in Hatch's solution (Figure 2B). Lung-phase Pb IVBA in unamended dust was lower compared to the results obtained for the SBRC-G assessment (<250 μm soil particle fraction) reported in the preceding section, which may be attributed to the lower pH of the latter. However, although IIBA-L and SBRC-I phases were conducted at neutral pH, IIBA-L Pb IVBA was 3.7-fold higher in the former. Lung surfactants and chelators in Hatch's solution may have rapidly transported the solubilized ions away from the surface of the dust particles, preventing their precipitation during IIBA-L assessment.(22) Additionally, the use of longer extraction period in IIBA-L (24 h) compared to SBRC-I (4 h) allowed a greater dissolution of Pb from the matrix, which was also observed in Kastury et al.(22) when assessing other mining/smelting impacted dusts.

In PA-, MAP-, and TSP-amended dust, Pb IVBA was significantly reduced from 61.7 ± 0.5% in the unamended dust to 20.0 ± 0.9% (PA) to 29.5 ± 1.1% (TSP) following assessment using IIBA-L ($p < 0.01$, TER = 0.33–0.48). In contrast, no significant reduction in Pb IVBA was observed in HA, bone meal biochar, and Fe_2O_3-amended dusts (TER = 0.9–1.1), presumably due to the reduced anglesite dissolution observed in IIBA-L residuals (Figure 2B). The presence of Pb phosphates in the MAP and TSP-amended IIBA-L residuals suggested the possibility that an outer layer of Pb phosphates may have formed surrounding Pb particles during the assay, reducing further Pb dissolution.(58)

5.2. Pb IVBA and Residual Pb Speciation Following IIBA Lung + Intestinal Phase (IIBA-I) Assessment

Following a 24 h extraction in lung fluid, dust particles were transitioned to gastric (pH 1.5, 1 h) and intestinal solutions (pH 7.0, 4 h) to simulate the clearance of particles from the lungs and their passage through the GI tract. In the unamended dust, Pb IVBA in IIBA-I was 74.5 ± 0.8% (Figure 2A). Solubilization of Pb in the acidic pH of the preceding gastric phase may be attributed to the higher Pb IVBA following IIBA-I extraction compared to IIBA-L,

which was also evident in the reduction in residual anglesite and an increase in residual plumbojarosites (Figure 2B). Similar to the SBRC-I phase, coprecipitation with Fe during the transition from IIBA-G to IIBA-I may be attributed to the increase in residual plumbojarosites.(37)

An important observation during the IIBA-L phase was that Pb IVBA was reduced from 74.5 ± 0.8% in the unamended dust to 44.9 ± 2.1% to 59.3 ± 1.8% in PA-, MAP-, and TSP-amended dust ($p < 0.01$, TER: 0.67–0.80), while no reduction was observed in HA-, biochar-, and Fe_2O_3-amended dust (TER 0.97–1.13). EXAFS analysis identified Pb phosphate species in the IIBA-I residuals of PA-, MAP-, and TSP-amended dust, which explains the reduction in Pb IVBA in the IIBA-I phase. The combined results of Pb IVBA reduction in phosphate-amended dust using IIBA-L and IIBA-I phases indicated that water-soluble phosphate amendments may be the most suitable for amending Pb-contaminated soil. This result is particularly germane in arid mining/smelting impacted regions of Australia, where exposure via aeolian transport of dust may be considered a significant contributor to childhood PbB.(19–21)

5.3 Pb Bioavailability Following Dust Instillation into Mouse Lungs

Based on the Pb IVBA results, unamended and PA-amended dust was instilled into mice lungs to ascertain whether a reduction in Pb absorption occurs *in vivo*. Reduction of inhalation bioavailability using phosphate amendment was deemed an important part of overall Pb exposure reduction in Broken Hill because studies using human subjects have demonstrated that up to 95% of the Pb in fine particles (<0.1 μm) may be absorbed upon inhalation.(59,60) A study conducted by Boreland et al.(21) reported an influx of 166–1104 μg of Pb/m^2 during a 30 day period, which indicated that windblown dust in an arid environment such as Broken Hill may potentially contribute to childhood PbB via inhalation. Although inhalation studies are preferrable for studying Pb absorption in ambient particulatte matter, the choice of instillation to assess Pb exposure as a surrogate to inhalation assays enabled a more precise delivery of small sample masses(19) compared to insufflation of dry dust, allowing direct comparison of Pb absorption in unamended and PA-amended dust. Following exposure to the unamended dust, PbB increased rapidly from 0.29 μg/L (time = 0) to 18.2 ± 4.4 at 0.25 h and 49.7 ± 5.1 μg/L after 2 h (Figure 2C). Subsequently, a slower rate of Pb absorption between 2 and 8 h resulted in a peak PbB of 80.1 ± 11.2 μg/L at 8 h. At the end of 24 h, a moderate decrease in PbB was observed (71.5 ± 9.8 μg/L). The rapid absorption of Pb from Pb contaminated dust in this study agrees with the results reported in Fent et al.,(19) who instilled dust from shooting range soil into rat lungs and reported high Pb absorption, which peaked at 24 h and slowly declined until 96 h without PbB returning to baseline. Although the maximum exposure time frame of 24 h in this experiment was not sufficiently long for PbB to return to baseline, this information, together with the biodistribution data obtained via the XRF images, yielded valuable insight into the bioavailability of Pb following exposure to Pb contaminated dust. Tricolor XRF images of lungs instilled with the unamended sample showed that Pb (red) became distributed throughout the lungs between 0.5–2 h (Figure 3A), presumably aided by gravity and lung surfactants.(61,62) While Fe (green) was mostly observed as associated with Pb (indicated by yellow), Ca (blue) was mostly observed in the upper respiratory tract,

incorporated in the tracheal rings. Metal sulfates (e.g., anglesite) have been suggested to be water-soluble and, therefore, potentially bioavailable in the lungs.(63,64) As anglesite was the predominant Pb phase in the unamended dust, anglesite dissolution may have resulted in the majority of Pb absorption via the air–blood barrier.

Tricolor images of the GI tracts showed that Pb appeared in the stomach 8 h post instillation with the unamended dust (Figure 4A), presumably due to particle clearance from the lungs by the mucociliary escalator and the diffusion of Pb throughout the stomach. This was confirmed by Pb concentrations in the lungs (Pb_L) and stomach (Pb_S) in Figure 4C where Pb_L decreased from 1.1 ± 0.2 μg/organ at 0.25 h to 0.5 ± 0.1 μg/organ at 8 h, while Pb_S increased from 0.06 ± 0.1 μg/organ at 0.25 h to 1.5 ± 0.3 μg/organ at 8 h. Low concentrations of Pb were detected in this compartment at 24 h (Figure 4A), presumably due to precipitation of non-absorbed Pb. Detection of Pb in the small intestinal tract suggested that, in addition to Pb absorption in the lungs, it is possible that a fraction of the PbB during 8–24 h resulted from the solubilization of Pb in the stomach, followed by absorption in the small intestine.(10)

In contrast to the unamended dust, PbB in mice instilled with PA-amended dust showed a slower rate of Pb absorption, with PbB at 0.25 h being 3.7 ± 0.5 μg/L and reaching a maximum of 48.7 ± 3.7 μg/L at 24 h (Figure 2C). A comparison of the AUC of the unamended and PA-amended dust suggested a 55.8 ± 1.6% decrease in the total Pb absorbed into the systemic circulation as a consequence of PA amendment over 24 h. Although it was not clear from Figure 3C whether PbB had peaked during 8–24 h or if it would continue to increase beyond 24 h, the reduction *in vivo* lies within the 32.4–67.5% reduction interval in the Pb IVBA using IIBA-L and IIBA-I phases. Additionally, because the reduced Pb absorption was more prominent during the first 8 h of the assay, it was theorized that similar to the Pb phosphates formation in the small intestine during the gavage study described above, Pb phosphates may have formed in the lung owing to its neutral pH. Further experiments with longer exposure time frames may be conducted to estimate AUC once PbB has returned to baseline with dose normalization using Pb acetate as a reference dose.

XRF images of lungs and GI tracts depict Pb dynamics in the PA-amended sample (Figures 3B and 4B). In contrast to the unamended dust, Pb particles from PA-amended dust were dispersed more rapidly at 0.25 h. The discrepancy between the dispersion rates most likely resulted from inter-animal variation, which is inherent in instillation experiments.(65) The quicker dispersion of PA-amended dust in the lungs may have contributed to its earlier detection in the stomach (4 h; Figure 4B). Pb_S increased from 0.41 ± 0.1 μg/organ at 0.25 h to 5.8 ± 1.6 μg/organ at 4 h and peaked at 11.1 ± 2.1 μg/organ after 8 h (Figure 4D), supporting the aforementioned suggestion that Pb from PA-amended dust demonstrated reduced absorption in the lungs.

To further test this theory, a 0.2 × 0.2 mm region of the lung receiving the unamended and PA-amended dust at 24 h was analyzed using XANES to investigate Pb speciation in the residual Pb particles. Within these regions, spectra corresponding to high and low Pb concentrations were obtained ($unamended_{high}$, $unamended_{low}$, $PA\text{-}amended_{high}$ and $PA\text{-}amended_{low}$, Figure S4). The spectra and their corresponding LCF fits are depicted in Figure

3C, while Pb speciation (weighted %) is provided in Figure 3D. Residual Pb speciation in the unamended$_{high}$ was dominated by anglesites (61.3%) with the remainder consisting of Pb phosphates (38.8%), while that in the PA-amended$_{high}$ was distributed as anglesite (48.5%) and Pb phosphates (51.5%), a 1.3 fold increase in Pb phosphates in the PA-amended dust residuals. Similarly, when residual Pb speciation in the unamended$_{low}$ and PA-amended$_{low}$ were assessed, a 1.3 fold increase in Pb phosphate was detected in the lungs receiving the PA-amended dust (39% in the unamended and 50.6% in the PA-amended). The remainder of the unamended$_{low}$ Pb was comprised of 51% anglesite and 10% mineral sorbed, while that in PA-amended$_{low}$ was 27.3% anglesite and 22.2% mineral sorbed. It is likely that similar to the results observed in the IIBA-L residuals, the Pb ions on the surface of anglesites reacted to P and Cl in the lung lining fluid forming a coating of chloropyromorphite, preventing subsequent dissolution, which was also reported in Wragg and Klinck during an IVBA study using SLF.(58) It is noteworthy that although a small region of the lung was analyzed for residual Pb speciation, the formation of Pb phosphates was 1.7 fold higher in the PA-amended dust. Therefore, it is possible that even though Pb phosphates did not form *in situ*, the presence of soluble P in the dust at the time of instillation increased the likelihood of Pb phosphate formation, thereby reducing Pb absorption in the lungs.

To the best of our knowledge, this is the first study to report a reduction of Pb exposure using phosphate-amended dust via instillation, however, a longer study may be required for PbB to return to (near) baseline. Nevertheless, this study highlighted that although P amendments with varying solubility reduced Pb exposure via the oral pathway, water-soluble amendments were more effective in immobilizing Pb via the inhalation pathway, with important implications of improving Pb exposure mitigation strategies worldwide. As particle retention in the lung is longer than that in the GI tract, future inhalation bioavailability studies should focused on longer term bioassays utilizing dust with different Pb phases to ascertain the influence of Pb speciation on Pb absorption in the lungs and GI tracts. Although the Pb concentration in urban soil is typically <1000 mg/kg, urban soil Pb has been linked with children's PbB.(66,67) Additionally, remediation of homes to seal houses to prevent Pb entry via fugitive dust has been shown to have limited impact on lowering children's PbB when initial Pb concentrations were not high.(20) Therefore, in urban soils and in arid regions, Pb immobilization using water-soluble phosphate sources may be an effective remediation strategy to mitigate Pb exposure.

Supplementary Material

Refer to Web version on PubMed Central for supplementary material.

Acknowledgements

The authors gratefully acknowledge the help of Susie Ritch, Ranju Karna, and Thea Read during the data analysis. Although the EPA contributed to this article, the research presented was not performed by or funded by the EPA and was not subject to the EPA's quality system requirements. Consequently, the views, interpretations, and conclusions expressed in this article are solely those of the authors and do not necessarily reflect or represent the EPA's views or policies. MRCAT operations are supported by the Department of Energy and the MRCAT member institutions.

References

1. WHO. Lead poisoning and health [Online early access] 2018 https://www.who.int/news-room/fact-sheets/detail/lead-poisoning-and-health.
2. Jusko TA; Henderson CR Jr; Lanphear BP; Cory-Slechta DA; Parsons PJ; Canfield RL Blood lead concentrations < 10 μg/dL and child intelligence at 6 years of age. Environ. Health Perspect 2008, 116, 243–248, DOI: 10.1289/ehp.10424 [PubMed: 18288325]
3. Lanphear BP; Hornung R; Khoury J; Yolton K; Baghurst P; Bellinger DC; Canfield RL; Dietrich KN; Bornschein R; Greene T Low-level environmental lead exposure and children's intellectual function: an international pooled analysis. Environ. Health Perspect 2005, 113, 894, DOI: 10.1289/ehp.7688 [PubMed: 16002379]
4. Surkan PJ; Zhang A; Trachtenberg F; Daniel DB; McKinlay S; Bellinger DC Neuropsychological function in children with blood lead levels < 10 μg/dL. NeuroToxicology 2007, 28, 1170–1177, DOI: 10.1016/j.neuro.2007.07.007 [PubMed: 17868887]
5. Chiodo LM; Jacobson SW; Jacobson JL Neurodevelopmental effects of postnatal lead exposure at very low levels. Neurotoxicol. Teratol 2004, 26, 359–371, DOI: 10.1016/j.ntt.2004.01.010 [PubMed: 15113598]
6. Zahran S; Laidlaw MA; McElmurry SP; Filippelli GM; Taylor M Linking source and effect: Resuspended soil lead, air lead, and children's blood lead levels in Detroit, Michigan. Environ. Sci. Technol 2013, 47, 2839–2845, DOI: 10.1021/es303854c [PubMed: 23428083]
7. Scheckel KG; Diamond GL; Burgess MF; Klotzbach JM; Maddaloni M; Miller BW; Partridge CR; Serda SM Amending soils with phosphate as means to mitigate soil lead hazard: a critical review of the state of the science. J. Toxicol. Environ. Health, Part B 2013, 16, 337–380, DOI: 10.1080/10937404.2013.825216
8. Zhao D; Wang J-Y; Tang N; Yin D-X; Luo J; Xiang P; Juhasz AL; Li H-B; Ma LQ Coupling bioavailability and stable isotope ratio to discern dietary and non-dietary contribution of metal exposure to residents in mining-impacted areas. Environ. Int 2018, 120, 563–571, DOI: 10.1016/j.envint.2018.08.023 [PubMed: 30172230]
9. Schultz A; Puvvadi R; Borisov SM; Shaw NC; Klimant I; Berry LJ; Montgomery ST; Nguyen T; Kreda SM; Kicic A Airway surface liquid pH is not acidic in children with cystic fibrosis. Nat. Commun 2017, 8, 1409, DOI: 10.1038/s41467-017-00532-5 [PubMed: 29123085]
10. Bannon DI; Drexler JW; Fent GM; Casteel SW; Hunter PJ; Brattin WJ; Major MA Evaluation of small arms range soils for metal contamination and lead bioavailability. Environ. Sci. Technol 2009, 43, 9071–9076, DOI: 10.1021/es901834h [PubMed: 20000496]
11. Kanapilly G; Raabe O; Goh C; Chimenti R Measurement of in vitro dissolution of aerosol particles for comparison to in vivo dissolution in the lower respiratory tract after inhalation. Health Phys 1973, 24, 497–507, DOI: 10.1097/00004032-197305000-00004 [PubMed: 4707664]
12. Nemmar A; Holme JA; Rosas I; Schwarze PE; Alfaro-Moreno E Recent advances in particulate matter and nanoparticle toxicology: a review of the in vivo and in vitro studies. BioMed Res. Int 2013, 2013, 1–22, DOI: 10.1155/2013/279371
13. Asgharian B; Menache M; Miller F Modeling age-related particle deposition in humans. J. Aerosol Med 2004, 17, 213–224, DOI: 10.1089/jam.2004.17.213 [PubMed: 15625813]
14. Rissler J; Gudmundsson A; Nicklasson H; Swietlicki E; Wollmer P; Löndahl J Deposition efficiency of inhaled particles (15–5000 nm) related to breathing pattern and lung function: an experimental study in healthy children and adults. Part. Fibre Toxicol 2017, 14, 10, DOI: 10.1186/s12989-017-0190-8 [PubMed: 28388961]
15. Hettiarachchi GM; Pierzynski GM Soil lead bioavailability and in situ remediation of lead-contaminated soils: A review. Environ. Prog 2004, 23, 78–93, DOI: 10.1002/ep.10004
16. Mele E; Donner E; Juhasz AL; Brunetti G; Smith E; Betts AR; Castaldi P; Deiana S; Scheckel KG; Lombi E In situ fixation of metal (loid) s in contaminated soils: a comparison of conventional, opportunistic, and engineered soil amendments. Environ. Sci. Technol 2015, 49, 13501–13509, DOI: 10.1021/acs.est.5b01356 [PubMed: 26457447]

17. Maddaloni M; Lolacono N; Manton W; Blum C; Drexler J; Graziano J Bioavailability of soilborne lead in adults, by stable isotope dilution. Environ. Health Perspect 1998, 106, 1589, DOI: 10.1289/ehp.98106s61589 [PubMed: 9860919]

18. Bradham KD; Diamond GL; Nelson CM; Noerpel M; Scheckel KG; Elek B; Chaney R; Ma Q; Thomas DJ Long term in situ reduction in soil lead bioavailability measured in the mouse model. Environ. Sci. Technol 2018, 52, 13908–13913, DOI: 10.1021/acs.est.8b04684 [PubMed: 30358995]

19. Fent GM; Evans TJ; Bannon DI; Casteel SW Lead distribution in rats following respiratory exposure to lead-contaminated soils. Toxicol. Environ. Chem 2008, 90, 971–982, DOI: 10.1080/02772240701782173

20. Boreland F; Lyle D Lead dust in Broken Hill homes: Effect of remediation on indoor lead levels. Environ. Res 2006, 100, 276–283, DOI: 10.1016/j.envres.2005.06.007 [PubMed: 16099450]

21. Boreland F; Lyle D; Wlodarczyk J; Balding W; Reddan S Lead dust in Broken Hill homes—a potential hazard for young children?. Aust N Z. J. Public Health 2002, 26, 203–207, DOI: 10.1111/j.1467-842X.2002.tb00674.x [PubMed: 12141613]

22. Kastury F; Smith E; Karna RR; Scheckel KG; Juhasz A An inhalation-ingestion bioaccessibility assay (IIBA) for the assessment of exposure to metal(loid)s in PM_{10}. Sci. Total Environ 2018, 631, 92–104, DOI: 10.1016/j.scitotenv.2018.02.337 [PubMed: 29524906]

23. El-Sherbiny IM; El-Baz NM; Yacoub MH Inhaled nano-and microparticles for drug delivery. Global Cardiol Sci. Pract 2015, 2, 1–14, DOI: 10.5339/gcsp.2015.2

24. Kastury F; Smith E; Juhasz AL A critical review of approaches and limitations of inhalation bioavailability and bioaccessibility of metal (loid) s from ambient particulate matter or dust. Sci. Total Environ 2017, 574, 1054–1074, DOI: 10.1016/j.scitotenv.2016.09.056 [PubMed: 27672736]

25. Bailey M; Ansoborlo E; Guilmette R; Paquet F Updating the ICRP human respiratory tract model. Radiat. Prot. Dosim 2007, 127, 31–34, DOI: 10.1093/rpd/ncm249

26. Wallenborn JG; Kovalcik KD; McGee JK; Landis MS; Kodavanti UP Systemic translocation of 70 zinc: kinetics following intratracheal instillation in rats. Toxicol. Appl. Pharmacol 2009, 234, 25–32, DOI: 10.1016/j.taap.2008.09.024 [PubMed: 18973770]

27. Solomon R The Richest Lode: Broken Hill 1983–1988; Hale & Iremonger: Sydney, 1988.

28. Yang K; Cattle SR Bioaccessibility of lead in urban soil of Broken Hill, Australia: a study based on in vitro digestion and the IEUBK model. Sci. Total Environ 2015, 538, 922–933, DOI: 10.1016/j.scitotenv.2015.08.084 [PubMed: 26363147]

29. Yang K; Cattle SR Effectiveness of cracker dust as a capping material for Pb-rich soil in the mining town of Broken Hill, Australia. Catena 2017, 148, 81–91, DOI: 10.1016/j.catena.2016.02.022

30. USEPA. Microwave assisted acid digestion of sediments, sludges, soils, and oils, 1998 https://www.epa.gov/sites/production/files/2015-12/documents/3051a.pdf

31. EPA. Method 6020A (SW-846): Inductively Coupled Plasma-Mass Spectrometry, Revision 1, 1998 https://www.epa.gov/sites/production/files/2015-07/documents/epa-6020a.pdf

32. Juhasz AL; Gancarz D; Herde C; McClure S; Scheckel KG; Smith E In situ formation of pyromorphite is not required for the reduction of in vivo Pb relative bioavailability in contaminated soils. Environ. Sci. Technol 2014, 48, 7002–7009, DOI: 10.1021/es500994u [PubMed: 24823360]

33. Kelley ME; Brauning S; Schoof R; Ruby M Assessing oral bioavailability of metals in soil; Battelle Press, 2002.

34. Berlinger B; Ellingsen DG; Náray M; Záray G; Thomassen Y A study of the bioaccessibility of welding fumes. J. Environ. Monit 2008, 10, 1448–1453, DOI: 10.1039/b806631k [PubMed: 19037486]

35. Kropf A; Katsoudas J; Chattopadhyay S; Shibata T; Lang E; Zyryanov V; Ravel B; McIvor K; Kemner K; Scheckel K: The new MRCAT (Sector 10) bending magnet beamline at the advanced photon source. In AIP Conference Proceedings; AIP, 2010; Vol. 1234; pp 299–302.

36. Clark JD; Gebhart GF; Gonder JC; Keeling ME; Kohn DF The 1996 guide for the care and use of laboratory animals. ILAR J 1997, 38, 41–48, DOI: 10.1093/ilar.38.1.41 [PubMed: 11528046]

37. Smith E; Kempson IM; Juhasz AL; Weber J; Rofe A; Gancarz D; Naidu R; McLaren RG; Gräfe M In vivo–in vitro and XANES spectroscopy assessments of lead bioavailability in contaminated

periurban soils. Environ. Sci. Technol 2011, 45, 6145–6152, DOI: 10.1021/es200653k [PubMed: 21707121]

38. Determination of heavy metals in whole blood by ICP-MS; Agilent Technologies Publication No. 5988–0533EN, 2006.
39. Cmielewski P; Farrow N; Devereux S; Parsons D; Donnelley M Gene therapy for Cystic Fibrosis: Improved delivery techniques and conditioning with lysophosphatidylcholine enhance lentiviral gene transfer in mouse lung airways. Exp. Lung Res 2017, 43, 426–433, DOI: 10.1080/01902148.2017.1395931 [PubMed: 29236544]
40. Ollson CJ; Smith E; Herde P; Juhasz AL Influence of co-contaminant exposure on the absorption of arsenic, cadmium and lead. Chemosphere 2017, 168, 658–666, DOI: 10.1016/j.chemosphere.2016.11.010 [PubMed: 27836265]
41. Etschmann BE; Donner E; Brugger J; Howard DL; de Jonge MD; Paterson D; Naidu R; Scheckel KG; Ryan CG; Lombi E Speciation mapping of environmental samples using XANES imaging. Environ. Chem 2014, 11, 341–350, DOI: 10.1071/EN13189
42. Gulson B; Mizon K; Taylor A; Wu M Dietary zinc, calcium and nickel are associated with lower childhood blood lead levels. Environ. Res 2018, 161, 87, DOI: 10.1016/j.envres.2017.10.040 [PubMed: 29102668]
43. Kordas K; Burganowski R; Roy A; Peregalli F; Baccino V; Barcia E; Mangieri S; Ocampo V; Mañay N; Martínez G Nutritional status and diet as predictors of children's lead concentrations in blood and urine. Environ. Int 2018, 111, 43–51, DOI: 10.1016/j.envint.2017.11.013 [PubMed: 29172090]
44. Calderon J; Navarro ME; Jimenez-Capdeville ME; Santos-Diaz MA; Golden A; Rodriguez-Leyva I; Borja-Aburto V; Diaz-Barriga F Exposure to arsenic and lead and neuropsychological development in Mexican children. Environ. Res 2001, 85, 69–76, DOI: 10.1006/enrs.2000.4106 [PubMed: 11161656]
45. Adamson I; Prieditis H; Hedgecock C; Vincent R Zinc is the toxic factor in the lung response to an atmospheric particulate sample. Toxicol. Appl. Pharmacol 2000, 166, 111–119, DOI: 10.1006/taap.2000.8955 [PubMed: 10896852]
46. Sneddon IR; Orueetxebarria M; Hodson ME; Schofield PF; Valsami-Jones E Field trial using bone meal amendments to remediate mine waste derived soil contaminated with zinc, lead and cadmium. Appl. Geochem 2008, 23, 2414–2424, DOI: 10.1016/j.apgeochem.2008.02.028
47. Brown S; Chaney R; Hallfrisch J; Ryan JA; Berti WR In situ soil treatments to reduce the phyto- and bioavailability of lead, zinc, and cadmium. J. Environ. Qual 2004, 33, 522–31, DOI: 10.2134/jeq2004.5220 [PubMed: 15074803]
48. Zhang P; Ryan JA Formation of pyromorphite in anglesite-hydroxyapatite suspensions under varying pH conditions. Environ. Sci. Technol 1998, 32, 3318–3324, DOI: 10.1021/es980232m
49. Carosino CM; Bein KJ; Plummer LE; Castañeda AR; Zhao Y; Wexler AS; Pinkerton KE Allergic airway inflammation is differentially exacerbated by daytime and nighttime ultrafine and submicron fine ambient particles: Heme oxygenase-1 as an indicator of PM-mediated allergic inflammation. J. Toxicol. Environ. Health, Part A 2015, 78, 254–266, DOI: 10.1080/15287394.2014.959627 [PubMed: 25679046]
50. Butkus MA; Johnson MC Reevaluation of Phosphate as a Means of Retarding Lead Transport from Sandy Firing Ranges. Soil Sediment Contam 2011, 20, 172–187, DOI: 10.1080/15320383.2011.546444
51. Debela F; Arocena JM; Thring RW; Whitcombe T Organic acid-induced release of lead from pyromorphite and its relevance to reclamation of Pb-contaminated soils. Chemosphere 2010, 80, 450–456, DOI: 10.1016/j.chemosphere.2010.04.025 [PubMed: 20444487]
52. Karna RR; Noerpel MR; Luxton TP; Scheckel KG Point of Zero Charge: Role in Pyromorphite Formation and Bioaccessibility of Lead and Arsenic in Phosphate-Amended Soils. Soil Syst 2018, 2, 22, DOI: 10.3390/soilsystems2020022 [PubMed: 30714024]
53. Juhasz AL; Scheckel KG; Betts AR; Smith E Predictive capabilities of in vitro assays for estimating Pb relative bioavailability in phosphate amended soils. Environ. Sci. Technol 2016, 50, 13086–13094, DOI: 10.1021/acs.est.6b04059 [PubMed: 27934280]

54. Scheckel KG; Ryan JA; Allen D; Lescano NV Determining speciation of Pb in phosphate-amended soils: Method limitations. Sci. Total Environ 2005, 350, 261–272, DOI: 10.1016/j.scitotenv.2005.01.020 [PubMed: 16227085]
55. Mercer KL; Tobiason JE Removal of arsenic from high ionic strength solutions: effects of ionic strength, pH, and preformed versus in situ formed HFO. Environ. Sci. Technol 2008, 42, 3797–802, DOI: 10.1021/es702946s [PubMed: 18546725]
56. Davis A; Ruby MV; Bergstrom PD Factors controlling lead bioavailability in the Butte mining district, Montana, USA. Environ. Geochem. Health 1994, 16, 147–157, DOI: 10.1007/BF01747911 [PubMed: 24197209]
57. Ruby M; Schoof R; Brattin W; Goldade M; Post G; Harnois M; Mosby D; Casteel S; Berti W; Carpenter M Advances in evaluating the oral bioavailability of inorganics in soil for use in human health risk assessment. Environ. Sci 1999, 33, 3697–3705, DOI: 10.1021/es990479z
58. Wragg J; Klinck B The bioaccessibility of lead from Welsh mine waste using a respiratory uptake test. J. Environ. Sci. Health, Part A: Toxic/Hazard. Subst. Environ. Eng 2007, 42, 1223–1231, DOI: 10.1080/10934520701436054
59. Hursh J; Schraub A; Sattler E; Hofmann H Fate of ^{212}Pb inhaled by human subjects. Health Phys 1969, 16, 257–267, DOI: 10.1097/00004032-196903000-00001 [PubMed: 5787740]
60. Wells A; Venn J; Heard M Deposition in the lung and uptake to blood of motor exhaust labelled with 203Pb. Inhaled Part 1975, 4, 175–189 [PubMed: 70403]
61. Brain JD; Knudson DE; Sorokin SP; Davis MA Pulmonary distribution of particles given by intratracheal instillation or by aerosol inhalation. Environ. Res 1976, 11, 13–33, DOI: 10.1016/0013-9351(76)90107-9 [PubMed: 1253768]
62. Geiser M; Kreyling WG Deposition and biokinetics of inhaled nanoparticles. Part. Fibre Toxicol 2010, 7, 1–17, DOI: 10.1186/1743-8977-7-2 [PubMed: 20180970]
63. Kyotani T; Iwatsuki M Determination of water and acid soluble components in atmospheric dust by inductively coupled plasma atomic emission spectrometry, ion chromatography and ion-selective electrode method. Anal. Sci 1998, 14, 741–748, DOI: 10.2116/analsci.14.741
64. Wallenborn JG; McGee JK; Schladweiler MC; Ledbetter AD; Kodavanti UPSystemic translocation of particulate matter–associated metals following a single intratracheal instillation in rats. Toxicol. Sci 2007, 98, 231–239, DOI: 10.1093/toxsci/kfm088 [PubMed: 17434951]
65. Kreyling WG; Hirn S; Möller W; Schleh C; Wenk A; Celik G. l.; Lipka J; Schäffler M; Haberl N; Johnston BD Air–blood barrier translocation of tracheally instilled gold nanoparticles inversely depends on particle size. ACS Nano 2014, 8, 222–233, DOI: 10.1021/nn403256v [PubMed: 24364563]
66. Mielke HW; Dugas D; Mielke PW, Jr; Smith, K. S.; Gonzales, C. Associations between soil lead and childhood blood lead in urban New Orleans and rural Lafourche Parish of Louisiana. Environ. Health Perspect 1997, 105, 950–954, DOI: 10.1289/ehp.97105950 [PubMed: 9300928]
67. Morrison D; Lin Q; Wiehe S; Liu G; Rosenman M; Fuller T; Wang J; Filippelli G Spatial relationships between lead sources and children's blood lead levels in the urban center of Indianapolis (USA). Environ. Geochem. Health 2013, 35, 171–183, DOI: 10.1007/s10653-012-9474-y [PubMed: 22782519]

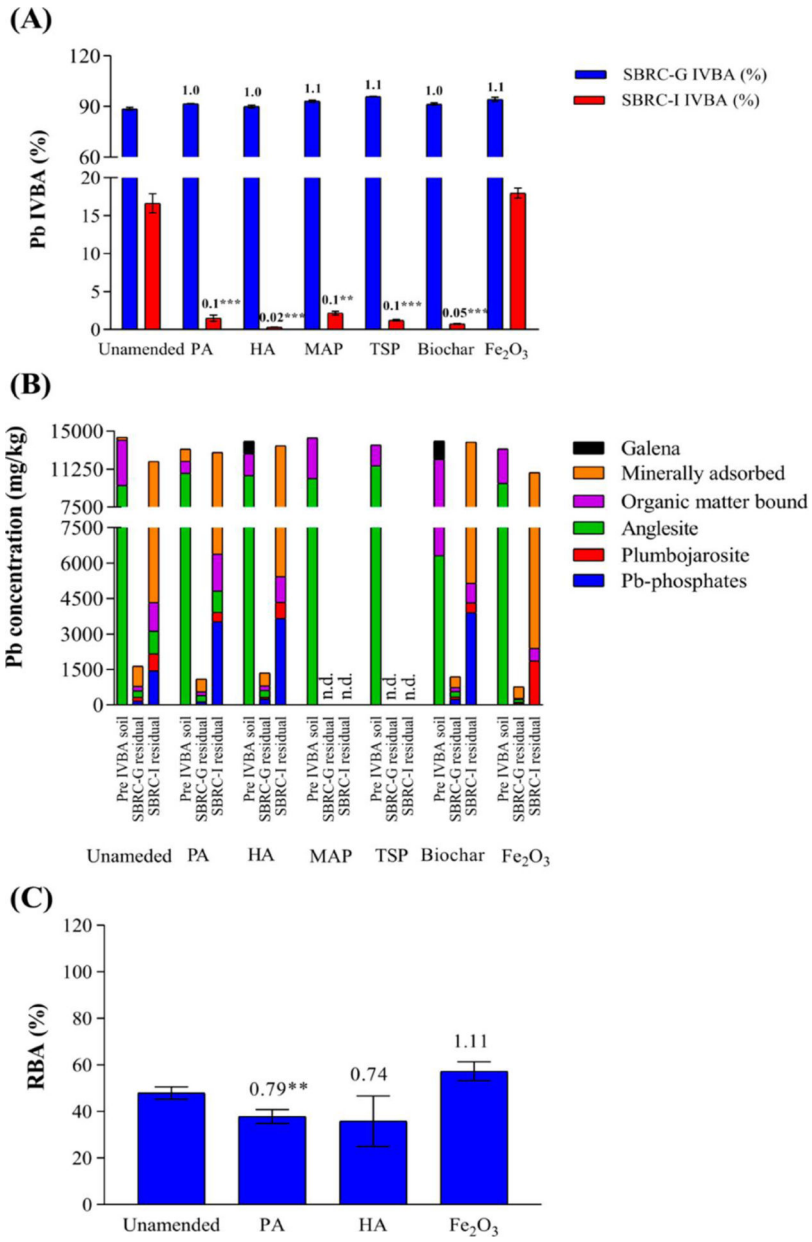

Figure 1.

(A) Pb IVBA (%) using the Solubility Bioaccessibility Research Consortium (SBRC) assay where SBRC-G = extraction using the gastric phase and SBRC-I = extraction using the small intestinal tract phase. (B) Pb speciation of pre- and post-SRBC assay residuals. (C) Pb relative bioavailability (RBA) in unamended and selected amended soil (PA = phosphoric acid, HA = hydroxyapatite, MAP = monoammonium phosphate, TSP = triple super phosphate). Numbers on the top of bars of (A) and (C) represent treatment effect ratio (TER). Asterix represents significance differences between unamended and amended soil (** = $p < 0.01$ and *** = $p < 0.001$) and n.d. = not determined.

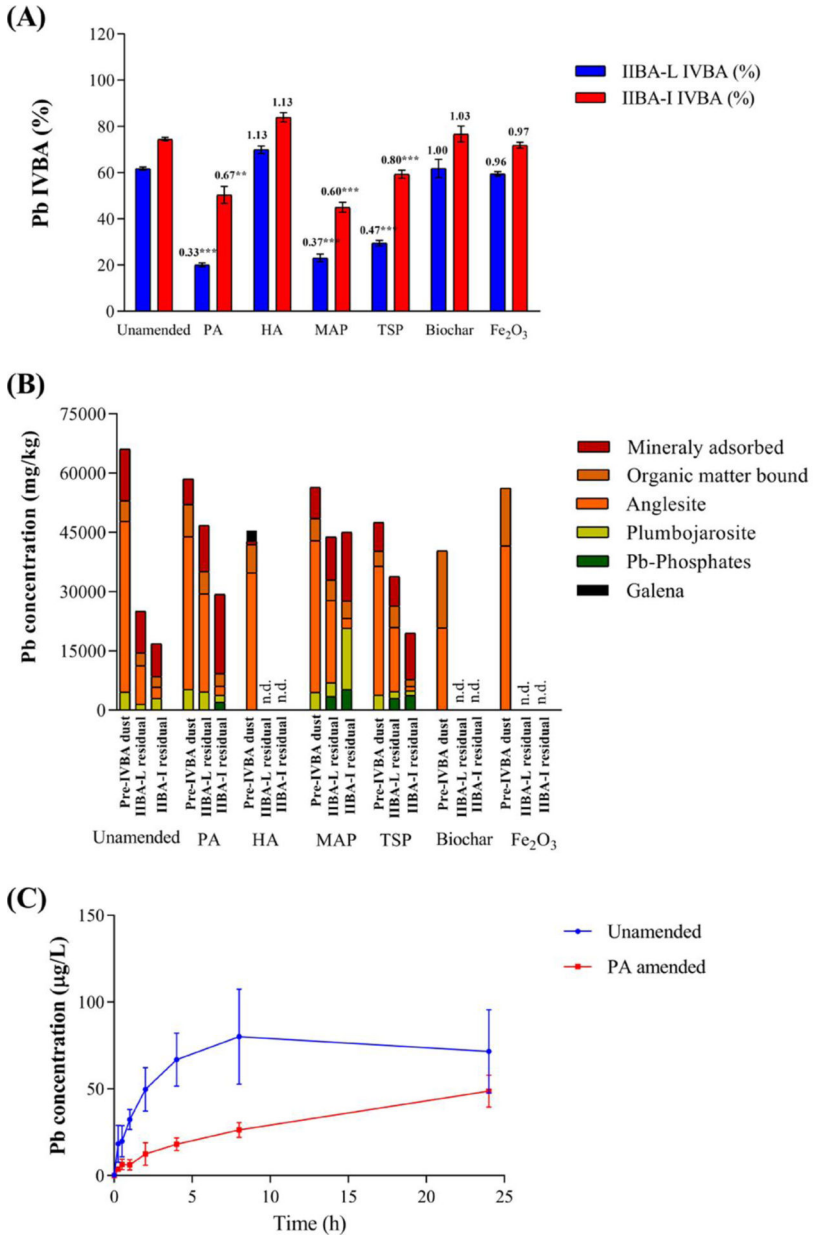

Figure 2.

(A) Pb IVBA (%) using the Inhalation–Ingestion Bioaccessibility Assay (IIBA) where IIBA-L = extraction using the lung phase, IIBA-I = extraction using the lung + small intestinal tract phase. (B) Pb speciation in pre- and post-IIBA assay residuals. (C) Blood Pb concentration following instillation of unamended and PA-amended soil (PA = phosphoric acid, HA = hydroxyapatite, MAP = monoammonium phosphate, TSP = triple super phosphate). numbers on the top of bars of (A) represent treatment effect ratio (TER). Asterix represents significance differences between unamended and amended soil (* = $p < 0.05$, ** = $p < 0.01$ and *** = $p < 0.001$) and n.d. = not determined.

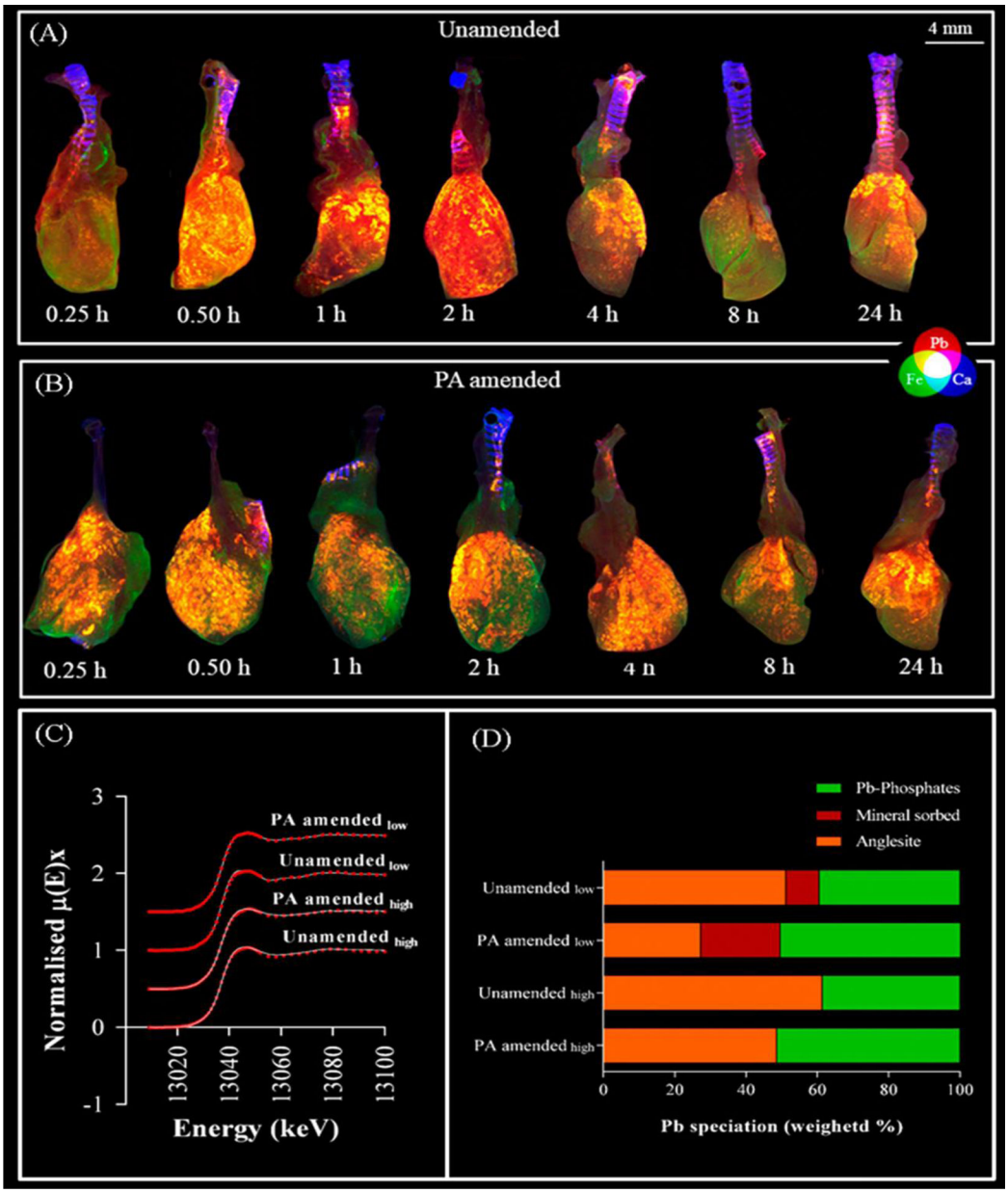

Figure 3.

(A, B) 2D Elemental map (Pb = red, Fe = green and Ca = blue) using X-ray fluorescence microscopy (XFM) in mice lungs (including partial trachea) exposed to unamended and phosphoric acid (PA) amended dust via instillation over 24 h. (C) Pb speciation in regions of interest in the 24 h mouse lungs using X-ray Absorption Near Edge Structures (XANES). Linear combination fitting (LCF) is indicated using red dots and original spectra as white lines. (D) Final Pb speciation (weighted %) results obtained using XANES

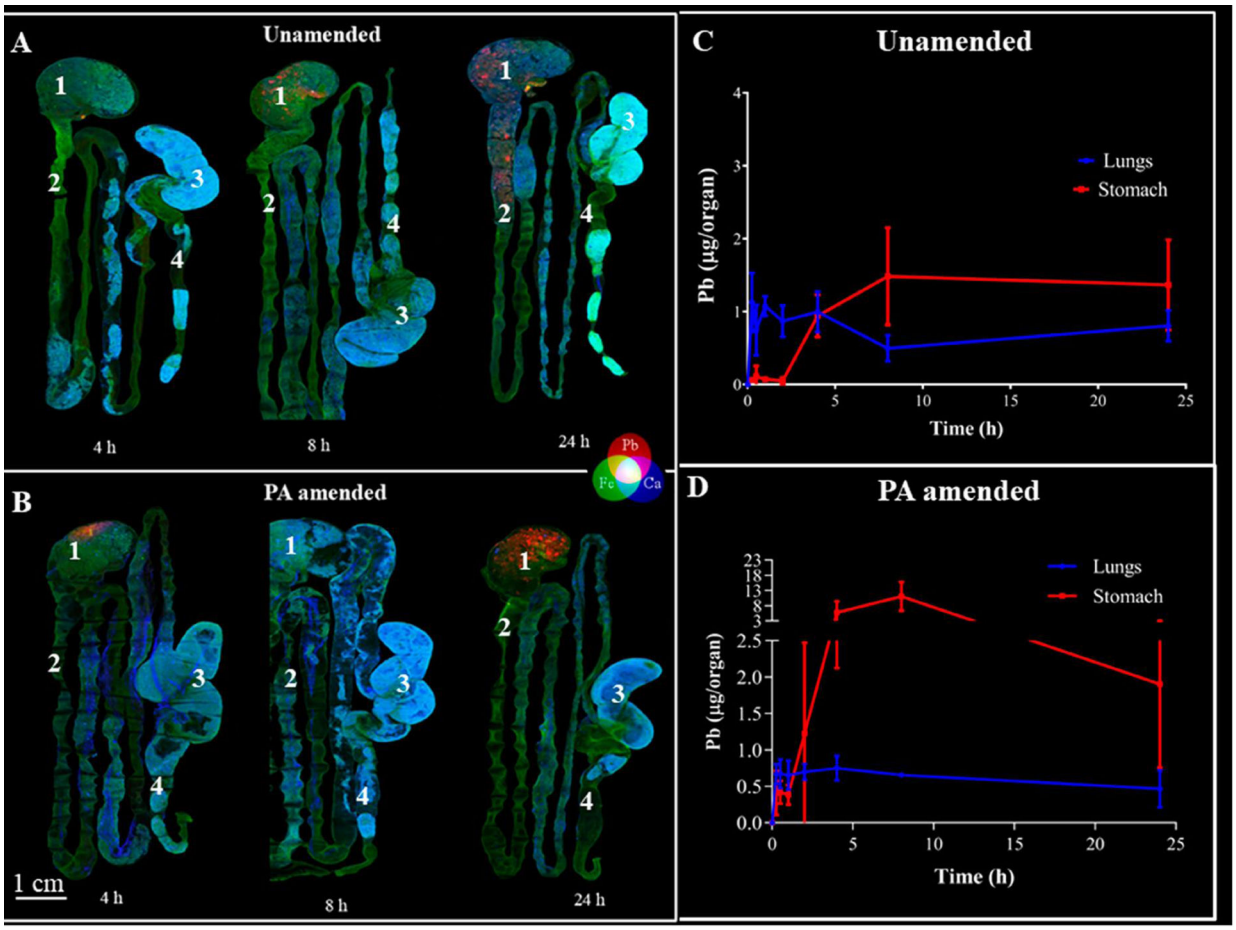

Figure 4.

(A, B) 2D Elemental mapping (Pb = red, Fe = green, and Ca = blue) in the gastro-intestinal (GI) tract of mice, 4–24 h post instillation with unamended and phosphoric acid (PA) amended dust (1, stomach; 2, small intestine; 3, cecum; 4, colon). (C, D) Pb concentration in lungs and stomach intestines between 0.25 and 24 h post instillation.

Table 1.

Physico-chemical Characterization of the Soil Particle Sizes Fractions and Amendments

			Minor element concentration (mean ± SEM) (mg/kg)			Major element concentration (mean ± SEM) (mg/kg)					
	pH	**Total organic carbon (%)**	**Pb**	**Mn**	**Zn**	**Al**	**Ca**	**Fe**	**K**	**Mg**	**P**
Total soil <2 mm	5.5±0.1	0.05±0.04	11656 ± 754	3337±305	5432±271	19035± 960	6202±367	25746±2140	5015±379	2760±182	712±55.5
Ingestible fraction <250 μm	ND[a]	ND[a]	14874±157	4223±190	6901±122	23412±706	8387±194	31807±311	5998±18.7	3273±12.5	855±39.9
Inhalable fraction <10 μm	ND[a]	ND[a]	62039±736	4171±6.8	18437±174	56359±2818	4207±57.9	73746±1049	11667±296	5036±51	1406±10.2

[a]ND = not determined.

Table 2.

Pb Speciation (wt %) in the <250 and <10 μm Soil Particle Fraction

	Adsorbed into clays and oxides	Organic matter bound	Anglesite ($PbSO_4$)	Plumbojarosite ($PbFe_6(SO_4)_4(OH)_{12}$)	Pb phosphates (pyromorphite + $Pb_3(PO_4)_2$)	Galena (PbS)	*R* factor
<250 μm soil particle fraction							
Unamended	2	31	67				0.001
PA	9	9	82				0.004
HA	0	16	78			6	0.004
MAP	0	28	72				0.001
TSP	0	15	85				0.003
Bonemeal biochar	0	42	45			13	0.006
Fe_2O_3	0	26	74				0.005
<10 μm soil particle fraction							
Unamended	20	8	66	7			
PA	11	14	66	9			
HA	2	24	74				0.003
MAP	14	10	68	8			
TSP	15	8	68	8			
Bonemeal biochar	0	44	44			12	0.005
Fe_2O_3	0	0	87		9	4	0.004

PA = phosphoric acid, HA = hydroxyapatite, MAP = monoammonium phosphate, TSP = triple super phosphate.